Dynamic Negative Compressibility of Few-Layer Graphene, h-BN, and MoS2

ARTICLE *in* NANO LETTERS · APRIL 2012

Impact Factor: 13.59 · DOI: 10.1021/nl300183e · Source: PubMed

9 AUTHORS, INCLUDING:

Helio Chacham
Federal University of Minas Gerais
124 PUBLICATIONS **2,031** CITATIONS
SEE PROFILE

Erlon Henrique Martins Ferreira
National Institute of Metrology, Quality and Te…
29 PUBLICATIONS **1,305** CITATIONS
SEE PROFILE

Ronaldo J. C. Batista
Universidade Federal de Ouro Preto
28 PUBLICATIONS **154** CITATIONS
SEE PROFILE

Bernardo R A Neves
Federal University of Minas Gerais
82 PUBLICATIONS **1,182** CITATIONS
SEE PROFILE

NANO LETTERS

Letter

pubs.acs.org/NanoLett

Dynamic Negative Compressibility of Few-Layer Graphene, h-BN, and MoS_2

Ana Paula M. Barboza,[†] Helio Chacham,[†] Camilla K. Oliveira,[†] Thales F. D. Fernandes,[†] Erlon H. Martins Ferreira,[‡] Braulio S. Archanjo,[‡] Ronaldo J. C. Batista,[§] Alan B. de Oliveira,[§] and Bernardo R. A. Neves*[,†]

[†]Departamento de Física, ICEx, Universidade Federal de Minas Gerais (UFMG), C.P. 702, 30123-970 Belo Horizonte, Brazil

[‡]Divisão de Metrologia de Materiais, Instituto Nacional de Metrologia, Normalização e Qualidade Industrial, 25250-020 Duque de Caxias, Brazil

[§]Departamento de Física, ICEB, Universidade Federal de Ouro Preto (UFOP), 35400-000 Ouro Preto, Brazil

S *Supporting Information*

ABSTRACT: We report a novel mechanical response of few-layer graphene, h-BN, and MoS_2 to the simultaneous compression and shear by an atomic force microscope (AFM) tip. The response is characterized by the vertical expansion of these two-dimensional (2D) layered materials upon compression. Such effect is proportional to the applied load, leading to vertical strain values (opposite to the applied force) of up to 150%. The effect is null in the absence of shear, increases with tip velocity, and is anisotropic. It also has similar magnitudes in these solid lubricant materials (few-layer graphene, h-BN, and MoS_2), but it is absent in single-layer graphene and in few-layer mica and Bi_2Se_3. We propose a physical mechanism for the effect where the combined compressive and shear stresses from the tip induce dynamical wrinkling on the upper material layers, leading to the observed flake thickening. The new effect (and, therefore, the proposed wrinkling) is reversible in the three materials where it is observed.

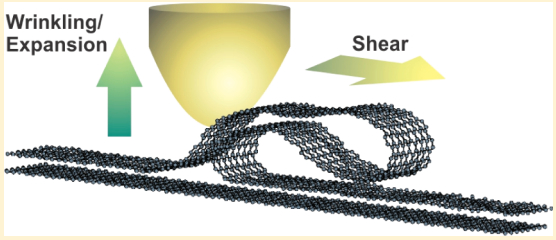

KEYWORDS: *Solid lubricants, negative compressibility, graphene, boron nitride, molybdenum disulfide, friction*

Graphite, hexagonal boron nitride (h-BN), and molybdenum disulfide (MoS_2) are known, for a long time, to be solid lubricants.[1] This partly arises from the weak bonding between adjacent layers in their crystal structure,[1,2] which enables the exfoliation down to single layers, leading to graphene[3] and to the h-BN and MoS_2 two-dimensional (2D) analogues.[4] These layered 2D materials may possess distinct physical properties, such as the relativistic-like electronic properties of graphene,[5,6] and unique tribological properties that are affected by the number of layers,[7,8] shear direction,[9] and the type of substrate.[10] In this Letter, we report a novel mechanical/tribological property observed in ultrathin films of solid lubricants (few-layer graphene, h-BN, and MoS_2): vertical expansion upon simultaneous vertical compression and shear applied by an external object. The stress/shear combination induces a dynamical wrinkling on the upper material layers, leading to a dynamic negative compressibility. Such effect is reversible and should occur universally during their lubricant action in conditions of everyday use.

As an external object to concomitantly apply (and control) compressive and shear stresses at the nanoscale, we employed an atomic force microscopy (AFM) tip operating in contact mode. Figure 1a–c shows three topographic AFM images of the same few-layer graphene flake where the tip load is progressively increased. The observed flake thickening, as it is compressed, is also evident in Figure 1d, which shows line profiles measured at the middle region of the flakes with increasing normal loads. It should be noted that Figure 1a–d indicates a negative compressibility of such few-layer graphene sample that results in strain values with an order of magnitude of a hundred percent, which is colossal in comparison with the strain values resulting from static negative compressibility, around tenths or hundredths percent, observed in some materials.[11] Like the static negative compressibility, the present effect is totally reversible: as soon as the applied load decreases, the measured thickness also decreases.

In order to test the universality of the new effect, four other layered materials were investigated besides graphene: hexagonal boron nitride (h-BN), molybdenum disulfide (MoS_2), mica, and bismuth selenide (Bi_2Se_3). The first two (h-BN and MoS_2) are, like graphite, materials that are solid lubricants in the bulk form[1] and can be mechanically exfoliated down to subnanometer layers.[3,4] In comparison, mica and Bi_2Se_3 can be exfoliated down to nanometer-thick layers[12,13] but are not solid lubricants in bulk form. Figure 2a shows the measured strain s (defined as $s = 1 - h/h_0$, where h is the measured flake

Received: January 15, 2012
Revised: March 29, 2012
Published: April 2, 2012

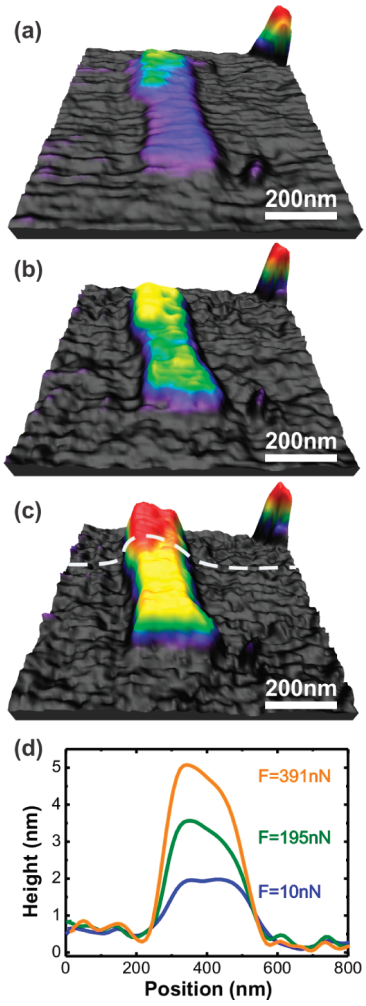

Figure 1. Negative compressibility effect. 3D-rendering topographic AFM images of the same graphene flake acquired in contact mode under increasing tip loads: (a) 10 nN, (b) 195 nN, and (c) 391 nN. (d) Height profiles taken from the images in (a), (b), and (c) evidencing the negative strain of the graphene flake (expansion upon compression). The dashed line in (c) indicates where the profiles were measured. The tip velocity was v = 5 μm/s.

thickness and h_0 is its initial thickness) as a function of applied normal load for all five materials. Initially, mica and Bi_2Se_3 show a small (but measurable) positive strain (compressibility); i.e., they shrink slightly upon compression. On the other hand, h-BN, MoS_2, and graphene exhibit similar and pronounced negative strain (expansion upon compression), where graphene presents the largest effect, followed by h-BN and MoS_2.

Following the results of Figure 2a, a natural question is whether this negative strain effect occurs for any number of layers in graphene, h-BN, and MoS_2. After analyzing tens of flakes of these materials, varying from monolayers to multilayers (up to ~20 nm thick), the results show that, even though its magnitude may vary, the effect always occurs for these three materials, regardless the number of layers, provided that there are at least two layers of the material. In other words, no negative compressibility effect is observed for a monolayer. Figure 2b illustrates this property: as shown in the inset of Figure 2b, a graphene flake consisting of a monolayer region (M) and a double-layer folded region (F) had its height (thickness) measured, via AFM-contact mode imaging, as a function of the applied normal load. Taking the SiO_2 substrate (S) as a reference, the relative heights of each part of the flake were measured: the fold height (F to S: black squares) increases as the normal force increases, characterizing the negative strain. On the other hand, the monolayer height (M to S: green triangles) decreases slightly upon compression, indicating a normal positive compressibility effect.

Measuring the folded-layer height relative to the monolayer, i.e., taking the monolayer as the reference (F to M: red circles), it is interesting to note that the negative strain effect is pronounced. In fact, adding both data sets, the folded-layer-to-monolayer height and the monolayer-to-substrate height ((F to M) + (M to S): orange triangles), produces exactly the folded-layer-to-substrate height data set. These results indicate that, experimentally, the negative compressibility is not a property of a single monolayer, but rather a collective effect of at least two, or more, monolayers. It should be noted, however, that such negative compressibility does not show a monotonic increase with the number of layers. In fact, data from tens of flakes indicate that the negative strain (the relative height variation) has a maximum for ~3−6 layers, as illustrated in Figure 2c. In this experiment, five graphene flakes with increasing thicknesses (from 1.7 nm up to 18.3 nm) had their negative compressibility effect measured. As the flake thickness increases, the relative thickness variation (or the slope of the curves in Figure 2c) decreases. In other words, in a thick flake (~20 nm or more), only the topmost 5−6 layers might contribute to the negative strain effect, with the other layers remaining unstrained or with a small positive strain.

The negative compressibility effect only exists if there is a combination of compressive stress and shear, as Figure 2d indicates. This figure shows how the relative thickness h/h_0 of graphene, h-BN, MoS_2, mica, and Bi_2Se_3 flakes varies with the tip scanning velocity for a constant normal load. While mica and Bi_2Se_3 thicknesses decrease as the tip speed increases, graphene, MoS_2, and h-BN show a pronounced increase of the negative compressibility effect as the tip velocity, and consequently the shear forces, increase (see Figure 3). For high speeds (>20 μm/s), there seems to be a saturation on the effect, which may coincide with the materials achieving their elastic deformation limits, since, at such speeds, the flakes are commonly torn up. Conversely, looking at the low speed region in Figure 2d, the negative strain effect should vanish at the zero velocity limit. In other words, if there is no shear, the negative strain effect is not produced. Such observation is corroborated by experiments where intermittent contact mode (or Tapping Mode) is used to image the flakes (see Supporting Information). Since there is no significant sample shear in this mode, the negative strain effect is not observed in any material.

The discussion in the last paragraph leads to the conclusion that the observed negative compressibility is a dynamic effect, induced not only by the compression of the flake by the tip but also by the shear forces created by the relative displacement of the tip on the topmost layers of such flake. Therefore, even though in the experiment a normal load is applied by the SPM tip, the lateral friction (shear) force between such tip and the topmost layer of the flake during their relative displacement is the relevant parameter. As a consequence, in order to investigate the shear behavior in the negative strain effect, additional experiments were carried out where contact mode is employed to perform lateral friction (or shear) force measurements. Because of the lack of a calibration standard, absolute friction forces were not measured, but only relative friction

dx.doi.org/10.1021/nl300183e | *Nano Lett.* 2012, 12, 2313−2317

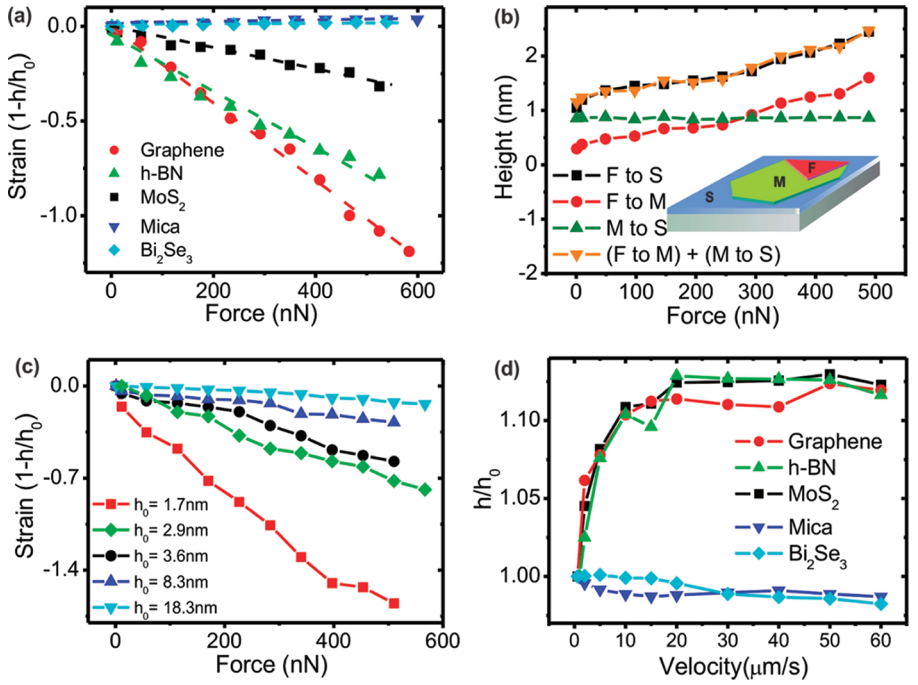

Figure 2. (a) Graph of the measured strain in different layered materials as a function of the applied normal tip load (graphene, ●; h-BN, ▲; MoS_2, ■; mica, ▼; Bi_2Se_3, ◆). The dashed lines are linear fits to the experimental data. The initial flake thicknesses, measured in Tapping Mode, are h_0(graphene) = 5.8 nm, h_0(h-BN) = 4.4 nm, $h_0(MoS_2)$ = 6.2 nm, h_0(mica) = 16.1 nm, and $h_0(Bi_2Se_3)$ = 24.6 nm. (b) Graph of the measured height as a function of applied force for different regions of a graphene flake, consisting of a monolayer (M) and a folded double-layer (F) regions atop the SiO_2 substrate (S), as illustrated in the inset. ■ and ▲ indicate the height of the few-layer and monolayer graphene with respect to the substrate, respectively. ● indicates the height of the few-layer region with respect to the monolayer, and ▼ represents the sum of the red and green data. (c) Negative strain effect in graphene flakes with different thicknesses h_0. v(tip) = 5 μm/s in (a), (b), and (c). (d) Graph of dependence of the relative height on the AFM tip scanning velocity for graphene (●), h-BN (▲), MoS_2 (■), mica (▼), and Bi_2Se_3 (◆) flakes. For all materials, the applied load was F = 170 nN. The lines in (b), (c), and (d) are just guides for the eye.

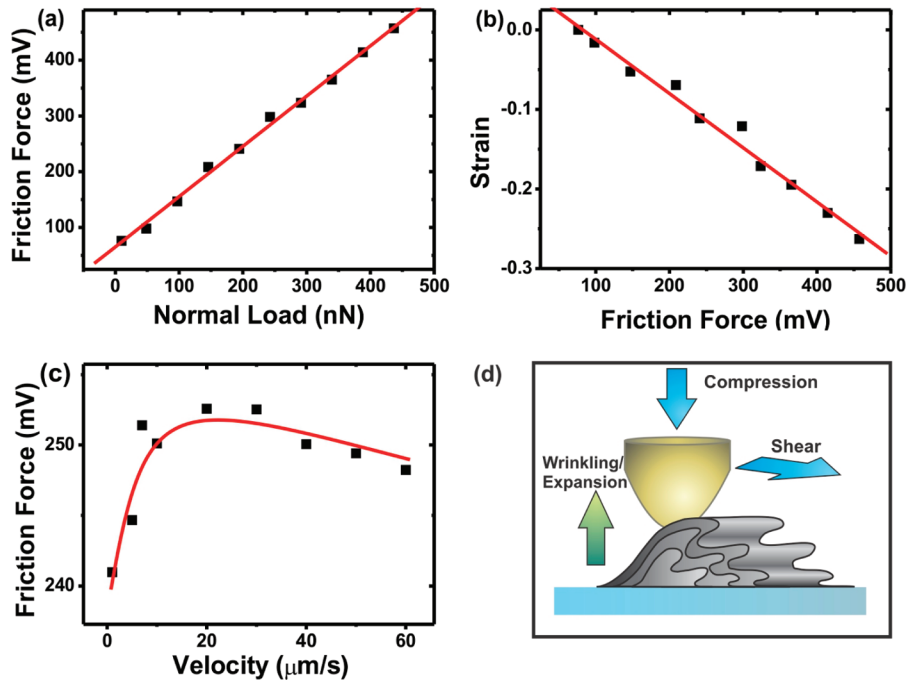

Figure 3. (a) Friction force measured as a function of applied normal load for a few-layer graphene flake. (b) Graphene flake strain measured as a function of the friction force. (c) Effect of tip velocity on the friction forces. (d) Cartoon illustrating the dynamic wrinkling mechanism that we propose for the dynamic compressibility effect. In the proposed mechanism, a few of the topmost layers of the material become folded/wrinkled in the region beneath the tip, as the tip moves, due to the shear (friction) force. The original, planar layered structure of the material is restored after the tip passes by the region.

dx.doi.org/10.1021/nl300183e | *Nano Lett.* 2012, 12, 2313−2317

forces (measured in the lateral photodetector units, mV), as commonly reported in the literature.[9] Figure 3 summarizes the main results. Initially, the friction force is measured as a function of applied normal load, for a few-layer graphene flake. As shown in Figure 3a, the friction force follows a linear relation with applied load (the well-known Amonton's law, which is also valid at the nanoscale[14,15]). Since the friction force increases with the applied load, a higher load should imply a larger shear, as assumed in the analysis of the results of Figure 2. Indeed, the graphene flake strain was measured as a function of the friction force as shown in Figure 3b. As expected, as the friction force increases, the negative strain also increases.

Finally, to enable a good comprehension of the data in Figure 2d, the effect of tip velocity on the friction forces was also measured (Figure 3c). Initially, the friction increases with tip velocity (under normal imaging velocities: $v < 10$ μm/s). At higher speeds ($v > 20$ μm/s), the friction saturates, and even decreases slightly, which, again, is in agreement with several reports in the literature.[15] This result explains the data in Figure 2d, which shows the strain behavior as a function of tip velocity for various materials: initially, as the tip velocity increases, so does the friction force. Therefore, the negative strain also increases. At high speeds, the friction force saturates (Figure 3c), and so should the negative strain (Figure 2d).

The results of Figures 2 and 3a–c suggest a dynamic/reversible wrinkling mechanism for the dynamic compressibility effect, as illustrated in the cartoon of Figure 3d. In the proposed mechanism, some of the topmost layers of the material (graphene, h-BN, or MoS_2) become folded/wrinkled in the region beneath the tip, as the tip moves, due to the shear (friction) force. Within the elastic deformation limit, the original planar layered structure of the material is restored after the tip moves away from the region. In other words, the observed negative compressibility effect is, indeed, a reversible friction-induced wrinkling/folding of the 2D layers. Such reversible wrinkling capability is intimately related to the lubricant properties of these three materials, i.e., the ability each single layer has to glide across another identical layer at low energy cost. Indeed, we have performed molecular dynamics simulations where a graphene layer atop another graphene layer is laterally compressed, producing folded/wrinkled configurations similar to those in Figure 3d (see Supporting Information). We shall also mention that static folds of similar nature have also been recently observed in graphene samples.[16] The gliding mechanism might also explain why mica and Bi_2Se_3, which are layered materials but not solid lubricants, due to a non-negligible interlayer interaction, do not present any negative compressibility. Additionally, it might even explain why the effect is not experimentally observed on supported monolayers atop a substrate. If the monolayer–substrate interaction were significant, as in the graphene–SiO_2 case, a very large shear force would be necessary to create the wrinkling process along the flake. In such a scenario, the AFM tip may tear up the monolayer flake and create a permanent fold, as observed experimentally for applied forces >500 nN[17] (see Supporting Information). A monolayer on a substrate with negligibly small interaction may be laterally displaced by the AFM tip as a whole, preventing any wrinkling. Therefore, in a way, an anchored first layer is needed to enable the gliding of the upper layers.

Being friction-dependent, the negative compressibility effect on graphene might suffer the effect of its crystallographic orientation. As recently proposed by Choi and collaborators, friction anisotropy exists on monolayer graphene, which could be associated to inhomogeneous interactions of graphene with the substrate and exhibited a 180° periodicity upon sample rotation.[9] Following this idea, one further experiment was carried out, as illustrated in Figure 4. Initially, a bilayer

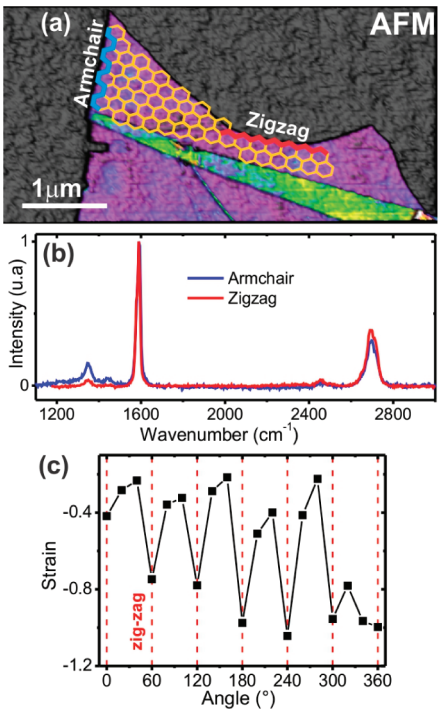

Figure 4. Crystallographic anisotropy of the dynamic negative compressibility effect. (a) Topographic AFM image of a bilayer graphene (in purple colors). The honeycomb lattice scheme is used to help the visualization of specific crystallographic edge orientations in this flake. (b) Raman spectra acquired at two edges of the flake, identified as armchair (blue line) and zigzag (red line). (c) Graph of the dependence of the negative compressibility effect on the rotation angle of the flake. The dashed red lines indicate wrinkling along the zigzag direction (ripple axis parallel to the armchair direction).

graphene flake with special edge geometry (shown in purple shades in the AFM image of Figure 4a) was found and investigated via polarized Raman spectroscopy, which enables the determination of zigzag and armchair edges.[18]

The Raman spectra of two special edges (shown in Figure 4b) unambiguously identify the blue spectrum in Figure 4b (blue edge in Figure 4a) as an armchair edge, whereas the red spectrum (red edge in Figure 4a) indicates a zigzag edge. After edge labeling, an angle-dependent negative compressibility experiment was performed: keeping the applied normal load and velocity constants ($F = 106$ nN and $v = 5$ μm/s), the flake was rotated by 360° (in steps of 20°), and the flake negative strain was measured for each angle, as shown in Figure 4c. The periodic nature of the negative strain effect is evident, with exactly 60° periodicity.

Following the edge labeling previously determined, one could also see that the zigzag direction produces the strongest negative compressibility effect (larger negative strain values). In other words, rastering the AFM tip along the zigzag direction induces graphene wrinkling more efficiently than along the armchair direction. This remarkable result may either indicate a larger tip–graphene friction coefficient along the zigzag direction, creating larger shear forces and inducing graphene

dx.doi.org/10.1021/nl300183e | Nano Lett. 2012, 12, 2313–2317

rippling more efficiently. Alternatively, the energy cost for wrinkling along the zigzag direction (wrinkle axis parallel to armchair direction) could be smaller than along the armchair direction. Nevertheless, the exact origin of such crystallographic anisotropy on the dynamic negative compressibility effect on graphene is beyond the scope of the present study and is left as a natural step forward in the investigation of these 2D materials (including h-BN and MoS_2; see Supporting Information).

Low-dimensional materials may present universal behaviors under mechanical deformation, such as, for example, the radial deformation of carbon nanotubes.[19] In such perspective, the dynamic negative compressibility effect described in this work could also be a universal property of all 2D-layered solid lubricants. Because of the wide applicability of such materials, from nanoelectromechanical systems to combustion engines, the precise understanding of the mechanisms of such effect may bring valuable improvements on the specification and operation of next-generation and present technology-based devices, from nano- to macroscales.

■ ASSOCIATED CONTENT

Supporting Information

Experimental and molecular dynamics simulation details, the effect of shear absence (in intermittent contact mode), the effect of substrate−flake interaction, the crystallographic anisotropy effect in other solid lubricants, the influence of intercalated water on few-layer graphene flakes, and the optimal conditions to observe the negative compressibility effect. This material is available free of charge via the Internet at http://pubs.acs.org.

■ AUTHOR INFORMATION

Corresponding Author

*E-mail: bernardo@fisica.ufmg.br.

Notes

The authors declare no competing financial interest.

■ ACKNOWLEDGMENTS

The authors are thankful to Prof. Carlos Achete, from Inmetro, for the use of the Raman Spectroscopy facilities, to Prof. Leandro Malard, from UFMG, for the MoS_2 and Bi_2Se_3 samples, to Dr. L. C. Campos and Prof. P. Jarillo-Herrero (MIT) for some graphene samples, and to Nacional de Grafite for providing high-quality crystals of natural graphite. A.P.M.B., C.K.O., and T.F.D.F. are thankful to CNPq for their scholarships. All authors acknowledge financial support from CNPq, Fapemig, Rede Nacional de Pesquisa em Nanotubos de Carbono, and INCT-Nano-Carbono.

■ REFERENCES

(1) Deacon, R. F.; Goodman, J. F. *Proc. R. Soc. London, Ser. A* **1958**, *243*, 464−482.
(2) Dickinson, R. G.; Pauling, L. *J. Am. Chem. Soc.* **1923**, *45*, 1466−1471.
(3) Novoselov, K. S.; Geim, A. K.; Morozov, S. V.; Jiang, D.; Zhang, Y.; Dubonos, I.; Grigorieva, I. V.; Firsov, A. A. *Science* **2004**, *306*, 666−669.
(4) Novoselov, K. S.; Jiang, D.; Schedin, F.; Booth, T. J.; Khotkevich, V. V.; Morozov, S. V.; Geim, A. K. *Proc. Natl. Acad. Sci. U. S. A.* **2005**, *102*, 10451−10453.
(5) Novoselov, K. S.; Geim, A. K.; Morozov, S. V.; Jiang, D.; Katsnelson, M. I.; Grigorieva, S. V.; Dubonos, S. V.; Firsov, A. A. *Nature* **2005**, *438*, 197−200.
(6) Zhang, Y.; Tan, Y.-W.; Stormer, H. L.; Kim, P. *Nature* **2005**, *438*, 201−204.
(7) Lee, C.; Li, Q.; Kalb, W; Liu, X.; Berger, H.; Carpick, R. W.; Hone, J. *Science* **2010**, *328*, 76−80.
(8) Filleter, T.; McChesney, J. L.; Bostwick, A.; Rotenberg, E.; Emtsev, K. V.; Seyller, T.; Horn, K.; Bennewitz, R. *Phys. Rev. Lett.* **2009**, *102*, 086102.
(9) Choi, J. S.; Kim, J; Byun, I.; Lee, D.; Park, B.; Lee, C.; Yoon, D.; Cheong, H.; Lee, K.; Son, Y.; Park, J. Y.; Salmeron, M. *Science* **2011**, *333*, 607−610.
(10) Kim, K.; Lee, C.; Lee, S.; Jang, H.; Ahn, J. K.; Lee, H. *ACS Nano* **2011**, *5*, 5107−5114.
(11) Aliev, A. E.; Oh, J.; Kozlov, M. E.; Kuznetsov, A. A.; Fang, S.; Fonseca, A. F.; Ovalle, R.; Lima, M. D.; Haque, M. H.; Gartstein, Y. N.; Zhang, M.; Zakhidov, A. A.; Baughman, R. H. *Science* **2009**, *323*, 1575−1578.
(12) Castellanos-Gomez, A.; Wojtaszek, M.; Tombros, N.; Agrait, N.; van Wees, B. J.; Rubio-Bollinger, G. *Small* **2011**, *7*, 2491−2497.
(13) Hong, S. S.; Kundhikanjana, W.; Cha, J. J.; Lai, K.; Kong, D.; Meister, S.; Kelly, M. A.; Shen, Z.; Cui, Y. *Nano Lett.* **2010**, *10*, 3118−3122.
(14) Mo, Y.; Turner, K. T.; Szlufarska, I. *Nature* **2009**, *457*, 1116−1119.
(15) Bhushan, B., Ed.; *Nanotribology and Nanomechanics: An Introduction*; Springer-Verlag: Berlin, 2008.
(16) Kim, K.; Lee, Z.; Molone, B. D.; Chan, K. T.; Aleman, B.; Regan, W.; Gannett, W.; Crommie, M. F.; Cohen, M. L.; Zettl, A. *Phys. Rev. B* **2011**, *83*, 245433.
(17) Carozo, V.; Almeida, C. M.; Ferreira, E. H. M.; Cançado, L. G.; Achete, C. A.; Jorio, A. *Nano Lett.* **2011**, *11*, 4527−4534.
(18) Cançado, L. G.; Pimenta, M. A.; Neves, B. R.; Medeiros-Ribeiro, G.; Enoki, T.; Kobayashi, Y.; Takai, K.; Fukui, K.; Dresselhaus, M. S.; Saito, R.; Jorio, A. *Phys. Rev. Lett.* **2004**, *93*, 047403.
(19) Barboza, A. P. M.; Chacham, H.; Neves, B. R. A. *Phys. Rev. Lett.* **2009**, *102*, 025501.